Binding of Cationic Porphyrin to Isolated DNA and Nucleoprotein Complex: Quantitative Analysis of Binding Forms under Various Experimental Conditions†

Kristóf Zupán,‡ Levente Herényi,‡ Katalin Tóth,§ Marianna Egyeki,‡ and Gabriella Csík*,‡

Institute of Biophysics and Radiation Biology, Semmelweis University, Budapest, Hungary, and Biophysik der Makromoleküle, DKFZ, Heidelberg, Germany

Received May 31, 2005; Revised Manuscript Received September 20, 2005

ABSTRACT: We studied the complex formation of tetrakis(4-*N*-methylpyridyl)porphyrin (TMPyP) with double stranded DNAs and T7 phage nucleoprotein complex. We analyzed the effect of base pair composition of DNA, the presence of capsid protein, and the composition of the microenvironment on the distribution of TMPyP between binding forms as determined by the decomposition of porphyrin absorption spectra. No difference was found in the amount of bound TMPyP between DNAs of various base compositions; however, the ratio of TMPyP binding forms depends on the AT/GC ratio. The presence of protein capsid opposes the binding of TMPyP to DNA. This behavior offers a possibility to investigate the protein capsid integrity due to the analysis of porphyrin binding. Increasing ionic strength of monovalent ions decreases the amount of bound porphyrin through the inhibition of intercalation, but does not influence the quantity of groove-binding forms when TMPyP interacts with isolated DNA. In the case of the nucleoprotein complex the groove-binding is also inhibited already at 140 mM ionic strength. The presence of 1 mM divalent cations (Mg^{2+}, Ca^{2+}, Cu^{2+} and Ni^{2+}) in a buffer solution of 70 mM ionic strength does not influence significantly the free to bound ration of TMPyP when it interacts with isolated DNA. The contribution of binding forms is remarkably different in Mg^{2+}/Ca^{2+} and Cu^{2+}/Ni^{2+} containing solutions. Transition metals significantly decrease the binding sites for intercalation in both DNA and nucleoprotein complex, but facilitate the groove-binding of TMPyP to isolated DNA.

The binding of cationic porphyrin derivatives to nucleic acids has been the subject of extensive research since Fiel and colleagues discovered that these compounds can form various complexes with DNA (*1*). Using UV/visible absorption (*2*, *3*) and fluorescence spectroscopy (*3*−*5*), circular and linear dichroism measurements (*3*, *6*), competition binding experiments (*7*), DNA footprinting (*8*), and molecular modeling (*8*−*10*) it has been shown that the binding can be either intercalative or external, in the minor groove (in some special cases with self-stacking), depending on the presence and the type of the central metal ion in porphyrin and on the peripheral substituents (*11*).

Given these biochemical properties, three main application fields of the cationic porphyrins have been developed in the past decade. These are the DNA-targeted photodynamic inactivation of microorganisms (*12*, *13*), the probing of the secondary and tertiary structure of nucleic acids (*14*, *15*), and the recognition of biomacromolecules using nanoparticles functionalized with cationic side chains (*16*, *17*). For these tasks, characterization of the environmental factors which influence the magnitude and the mode of the DNA-binding is particularly important. Among those factors, the effect of the ionic strength (*18*, *19*) and the base pair composition (AT/GC ratio) of DNA (*20*, *21*) have been documented.

The binding constants of TMPyP[1] to homogeneous DNAs have been determined under various experimental conditions (*19*). The binding constant with natural polynucleotide calf thymus DNA has been also estimated by several authors; however, the technique used earlier gave only a global apparent binding constant irrespective of the mode of binding to DNA (*22*, *23*). Moreover, the binding of cationic porphyrins to nucleoprotein complexes has not been analyzed before. However, for the design of certain applications of cationic porphyrins, such as the photoinactivation of viruses or molecular recognition of various DNA sequences, not only the amount of bound porphyrin but also the expected concentration of specific binding modes can be critically important.

Recently, we described a method (*24*), based on the decomposition of the Soret band of porphyrin absorption spectra, which facilitates the identification and quantitative characterization of tetrakis(4-*N*-methylpyridyl)porphine (TMPyP) binding forms even in their mixtures, as they are when TMPyP binds to natural DNA.

The aim of the present work is the quantitative analysis of intercalative and groove binding forms of tetrakis(4-*N*-methylpyridyl)porphine under various experimental condi-

† Supported by Grants NATO LST/CLG 977846, ETT 083/2003, and DAAD/PPP/12/2004.

* To whom correspondence should be addressed. Mailing address: 1444 Budapest POB 263. Phone/fax: 36-1-266-6656. E-mail: csik@puskin.sote.hu.

‡ Semmelweis University.

§ DKFZ.

[1] Abbreviations: NP, phage nucleoprotein complex; SDS, sodium dodecylsulfate; TMPyP, meso-tetrakis(4-*N*-methylpyridyl)porphyrin; TRIS, tris(hydroxymethyl)aminomethane.

10.1021/bi0510227 CCC: $30.25
Published on Web 10/22/2005

Table 1: Composition and Ionic Strength (μ) of Tris-HCl Buffer Solutions

μ (mM)	Tris-HCl (mM)	NaCl (mM)
67	20	50
135	40	100
195	40	160
395	40	360

tions. Using our method presented before, we determine the relative quantity of intercalative and groove-binding forms as a function of the ionic strength and composition of the buffer solution, of temperature, and of the AT/GC ratio of natural polynucleotide. Moreover, we attempt to track the effect of the higher-order structural changes of the polynucleotide when transforming from its encapsidated to its native form.

MATERIALS AND METHODS

meso-Tetrakis(4-N-methylpyridyl)porphyrin was purchased from Porphyrin Products. It was stored at 4 °C in powder form or as a stock solution in distilled water. Before experiments it was diluted to buffer solution composed of 20 mM Tris-HCl and 50 mM NaCl adjusted to pH = 7.4. Deoxyribonucleic acid isolated from *Micrococcus luteus* (*lysodeikticus*) (Sigma-Aldrich, Germany) and from chicken erythrocyte (Reanal, Hungary) was stored at 4 °C in powder form or as a stock solution in distilled water. Before experiments they were dialyzed against buffer solution described above. The typical length of DNA fragments was 10−20 kbase pair, as it was checked by gel electrophoresis.

Composition of Tris-HCl buffer solutions of various ionic strengths (μ) are summarized in Table 1. Divalent cations Ca^{2+}, Cu^{2+}, Ni^{2+} were added to Tris-HCl buffer of 70 mM ionic strength.

T7 bacteriophage (ATCC 11303-B7) was grown on *Escherichia coli* (ATCC 11303) host cells. Cultivation and purification were carried out according to the method of Strauss and Sinsheimer (*25*). The phage suspension was concentrated on a CsCl gradient and dialyzed against Tris-HCl buffer (pH = 7.4) of 70 mM ionic strength (*26*). The concentration of T7 bacteriophage was determined from its optical density using a molar absorptivity of $\epsilon_{260} = 7.3 \times 10^3$ (mol nucleotide bases·L^{-1}·cm^{-1}) in phosphate buffer.

Preparation of DNA. DNA was prepared from phages by incubating with 0.5% SDS (Sigma) for 30 min at 65 °C; then the protein−SDS complex was precipitated with 1 M KCl (Sigma) on ice for 10 min (*27*). The precipitate was centrifuged twice for 10 min in an Eppendorf microcentrifuge at 13 000 rpm, and the DNA was precipitated with ethanol from the supernatant. The pellet was washed with 70% ethanol and suspended in buffer solution, 20 mM Tris-HCl and 50 mM NaCl, pH = 7.4, and the amount of DNA was determined spectrophotometrically. The quality of DNA was checked by electrophoresis and by its absorption spectrum.

Absorption Spectroscopy. Ground-state absorption spectra of TMPyP solutions were recorded with 1 nm steps and 2 nm bandwidth by use of a Cary 4E (Varian, Mulgrave, Australia) spectrophotometer at various DNA or NP concentrations. The composition of solutions was expressed in terms of an *r* number representing the molar ratio of DNA base pairs to TMPyP molecules. Spectral changes due to the adsorption or aggregation of porphyrin were not taken into consideration because the adsorption of TMPyP on the cuvette wall was less than 5% during 30 min and the free porphyrin was in the monomeric state in all samples.

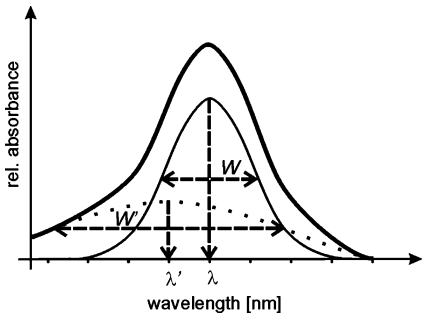

FIGURE 1: Schematic interpretation of spectral decomposition of TMPyP absorption spectrum between 390 and 480 nm: absorption spectrum of one state [$A_X(\lambda)$] (bold line) and its component spectra, main band [$A_x(\lambda)$] (thin line) and its shoulder [$A'_x(\lambda)$] (dotted line). Spectral parameters: The width (w and w') and center of the peak (λ and λ') are indicated.

Decomposition of Absorption Spectra. Absorption spectra of TMPyP bound to DNA or NP were analyzed with the method described before (*24*). Briefly, the spectral decomposition was performed for absorption spectra [$A(\lambda)$, absorbance versus wavelength] of the series of TMPyP−DNA and TMPyP−NP solutions with various base pair/porphyrin molar ratios (r). All of the spectra were analyzed in the 390−480 nm wavelength range.

For fitting we used the Gaussian multipeak fit routine from the Microcal Origin software. The error of the fit was determined as

$$\chi^2 = \frac{\sum_{\lambda=390}^{480} [A(\lambda)_{\text{measured}} - A(\lambda)_{\text{calculated}}]^2}{\sum_{\lambda=390}^{480} A(\lambda)_{\text{measured}}} \quad (1)$$

For further analysis of absorption spectra we made the following assumptions:

(1) All of the measured spectra [$A(\lambda)$] can be considered as a sum of three component spectra belonging to three possible porphyrin states, namely, to free [$A_F(\lambda)$], to externally bound [$A_E(\lambda)$], and to intercalated [$A_I(\lambda)$] porphyrins:

$$A(\lambda) = A_F(\lambda) + A_E(\lambda) + A_I(\lambda) \quad (2)$$

(2) The spectrum of each state [$A_X(\lambda)$] can be fitted as a sum of two Gaussians, a band [$A_x(\lambda)$] and its shoulder [$A'_x(\lambda)$] (see Figure 1):

$$A_X(\lambda) = \frac{A_x}{w_x\sqrt{\pi/2}} \exp\left(\frac{-2(\lambda - \lambda_x)^2}{w_x^2}\right) + \frac{A'_x}{w'_x\sqrt{\pi/2}} \exp\left(\frac{-2(\lambda - \lambda'_x)^2}{w'^2_x}\right) \quad (3)$$

A_x and A'_x are the total areas under the curves; λ_x and λ'_x are the centers of the peaks; w_x and w'_x are the full widths for the band and for the shoulder, respectively.

Table 2: Parameters of the Absorption Spectra of TMPyP Species[a]

	λ_x (nm)	w_x (nm)	λ_x' (nm)	w'_x (nm)	α_x	ϵ (M^{-1} cm^{-1})
free	423	17	415	41	1.32	3.17×10^5
DNA model						
external binding	430	20	420	67	1.20	2.98×10^5
intercalation	446	19	420	67	0.80	1.66×10^5
NP model						
external binding	430	20	411	73	1.29	2.29×10^5
intercalation	446	19	411	109	1.59	1.34×10^5

[a] Centers (λ_x, λ_x') and widths (w_x, w'_x) of main absorption bands and shoulder; ratio of areas under shoulder and main band (α_x), and molar absorptivities at the maximum of the spectrum (ϵ).

(3) The ratio of A'_x to A_x is constant at different populations of one state and can be expressed as

$$\alpha_x = A'_x/A_x \quad (4)$$

Table 2 shows α_x values determined in our previous work (*24*). The spectral parameters of TMPyP species and corresponding molar absorptivities at the maximum of the spectrum (ϵ) are also presented in Table 2.

RESULTS AND DISCUSSION

Influence of DNA Structure. In our previous work (*24*) we proved the presence of two main binding types of TMPyP, i.e., external binding and intercalation both in free and in encapsidated DNA. However, the spectral properties of bound species, especially those of externally bound forms, were found to be different in the case of two DNA conformations (see Table 2). TMPyP−DNA and TMPyP−NP complexes can be analyzed using "DNA model" and "NP model", respectively. Here we aim to provide further evidence for the role of DNA structure in the TMPyP−nucleic acid interaction.

A solution of TMPyP was prepared and completed with T7 NP to get a base pair/porphyrin ratio $r = 5$. Absorption spectra of this solution were recorded at various temperatures between 20 and 70 °C. Using NP model, the relative concentration of TMPyP species and the fitting errors (χ^2) were determined. As it is presented in Figure 2A, at room temperature most of the TMPyP molecules are in free state if $r = 5$. Between 40 and 60 °C a significant redistribution of TMPyP can be observed. The relative contribution of both bound species gradually increases, and the complete binding is reached when the temperature is as high as 60 °C.

Parallel to the temperature dependent redistribution of TMPyP, a significant increase in the fitting error can be recognized indicating the increasing inaccuracy of fitting procedure (Figure 2B). The opposite tendency can be observed in the changes of χ^2 if the whole spectral analysis is made with DNA model (data not shown).

A similar experiment and spectral analysis was made with TMPyP and isolated T7 DNA. The results presented in Figure 2C and 2D show that the temperature has a little effect on the TMPyP complexation to isolated DNA.

The temperature dependent complexation of TMPyP to encapsidated DNA can be explained by the corresponding structural changes of T7 nucleoprotein. A phase transition of the phage particles takes place between 50 and 60 °C, as it has been shown first by electron microscopy (*28*) and confirmed later in solution by the observed decrease in light scattering intensity (*29*). During this transition, the DNA is released from the capsid; it adopts a regular B tertiary structure and loses its higher order arrangement (*30*). Under this phase transition temperature TMPyP interacts with truly encapsidated DNA of distorted B conformation; above that temperature a binding between TMPyP and free DNA takes place. This is indicated not only by the redistribution of TMPyP around the phase transition temperature but also by the fitting errors obtained with the application of two different binding models.

Influence of DNA Base Composition. To analyze the role of DNA base composition in the TMPyP binding, three natural DNAs of different GC/AT ratios, namely, DNA from *M. luteus*, from T7 phage, and from chicken erythrocyte, have been investigated. Their GC contents are 72%, 50% and 42%, respectively.

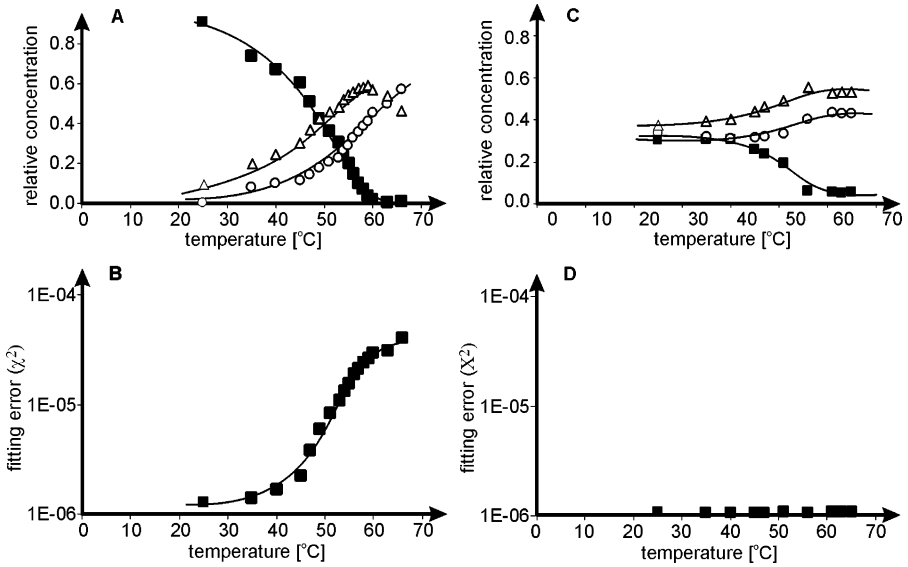

FIGURE 2: Effect of temperature on the TMPyP binding to T7 nucleoprotein complex (A) and isolated T7 DNA (C): relative concentration of free (■), intercalated (○), and externally bound (△) TMPyP as a function of the temperature. The base pair/porphyrin ratio was 5; spectra were recorded in TRIS buffer of 67 mM ionic strength. Panels B and D present the error of the fitting process (χ^2) in the case of T7 nucleoprotein complex and isolated T7 DNA received with the application of NP model and DNA model, respectively.

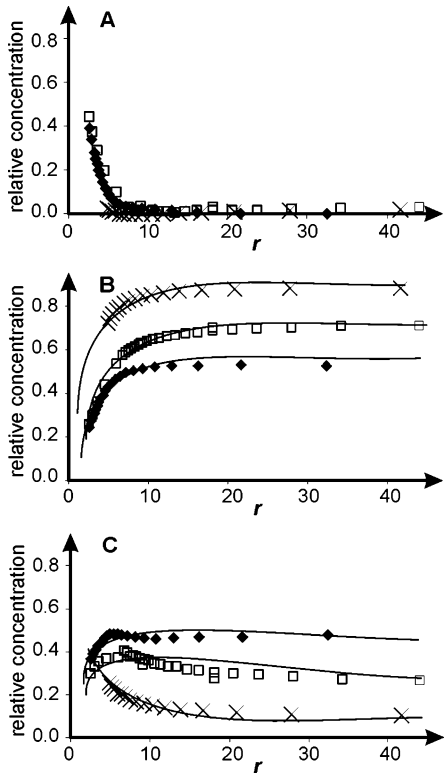

FIGURE 3: Binding of TMPyP to DNA isolated from chicken erythrocyte (◆), T7 phage (□), and *Micrococcus luteus* (×): relative concentration of free (A), intercalated (B), and externally bound (C) TMPyP as a function of the base pair/porphyrin ratio (*r*). Spectra were recorded in TRIS buffer of 67 mM ionic strength.

As the spectral analysis shows, there is no difference between DNAs of various base compositions as far as the total amount of bound TMPyP is concerned (Figure 3A). However, the distribution of TMPyP between binding forms depends on the base composition. According to our analysis the higher GC content discriminates in favor of intercalation against groove binding (Figure 3B). As the data in Figure 3C shows, the relative concentration of groove binding species increases with GC content.

The problem of sequence specificity of the binding of cationic porphyrins to DNA has been investigated by several authors (*4*, *10*, *20*, *31*). Our results fit to the general view that the binding of AT regions is nonintercalative, whereas that to GC has been defined as intercalative.

Effect of the Ionic Strength of Monovalent Ions. An important question regarding the binding of porphyrins to nucleic acids is that of the influence of ionic strength.

Absorption spectra of TMPyP−DNA and TMPyP−NP complexes were recorded in TRIS buffers of various ionic strengths from 70 to 400 mM. Relative concentrations of TMPyP binding forms were determined by the analysis of the spectra.

Figure 4A−C presents the relative concentration of free, intercalated, and externally bound TMPyP in the presence of isolated T7 DNA. As it is expected, the increase of the ionic strength opposes the binding of TMPyP to DNA. In 70 mM ionic strength buffer a complete TMPyP binding can be observed if $r > 10$. When $\mu = 140$ mM, the same binding level can be reached only at $r > 20$. Further increase in ionic strength drastically decreases the amount of bound TMPyP:

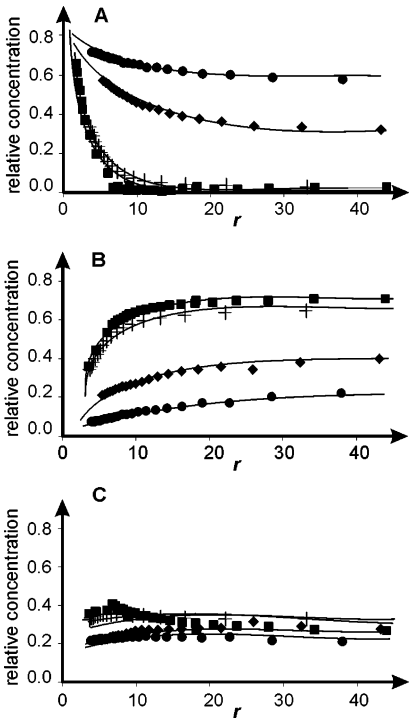

FIGURE 4: Binding of TMPyP to isolated T7 DNA: relative concentration of free (A), intercalated (B), and externally bound (C) TMPyP as the function of the base pair/porphyrin ratio (*r*) in TRIS buffer of 67 (■), 135 (+), 195 (◆), and 395 (●) mM ionic strength.

in the solution of $\mu = 200$ mM about 35% of the total TMPyP is free even at $r = 70$.

The increase of free to bound proportion with increasing ionic strength originates from the depletion of intercalated TMPyP species. In 70 mM ionic strength buffer 70% of total porphyrin is in intercalated state around the saturation of the binding process, and only 30% of that is externally bound. In 200 mM ionic strength buffer the intercalation is reduced to 40%; meanwhile, the change in the externally bound concentration is not significant.

Our results correspond to several earlier observations in this field. Previous works demonstrated that the binding of TMPyP to nucleic acids becomes weaker as the bulk ionic strength increases (*18*, *19*). Moreover, a shift from intercalation to the externally bound form was also noted at higher salt concentrations (*11*, *18*).

This can be interpreted as the result of structural changes both in DNA and in TMPyP molecules. It has been shown (*32*) that the DNA structure is stabilized by the increasing ionic strength. This is indicated by the increasing phase transition temperature corresponding to the DNA unwinding parallel to concentration of monovalent salts between 100 and 200 mM ionic strength. On the other hand, decreasing unwinding angles of TMPyP molecules in high ionic strength environment have been also proved by Geacintov et al. (*6*).

The binding is also inhibited by the increasing ionic strength when TMPyP interacts with NP; however, the change in the distribution of binding forms is different as it is shown in Figure 5A−C. Out of the reduction of intercalated TMPyP concentration already at 140 mM ionic strength, a significant decrease in the number of external binding sites can be also observed up to $\mu = 200$ mM. These results indicate that not only DNA and TMPyP structure but also

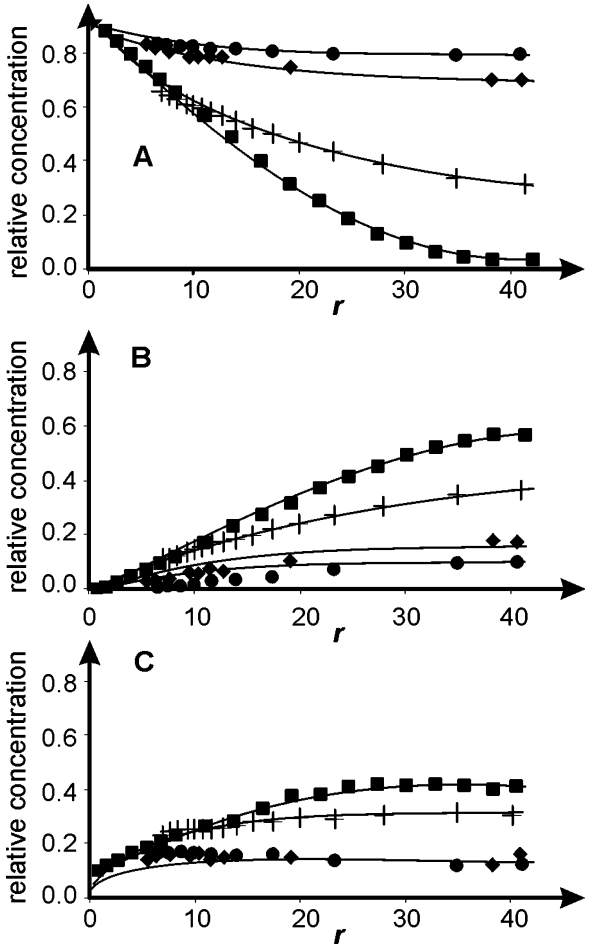

FIGURE 5: Binding of TMPyP to T7 nucleoprotein complex: relative concentration of free (A), intercalated (B), and externally bound (C) TMPyP as the function of the base pair/porphyrin ratio (r) in TRIS buffer of 67 (■), 135 (+), 195 (◆), and 395 (●) mM ionic strength.

the protein capsid stability and/or DNA−protein interaction are altered in this ionic strength range. This is also supported by the results of Toth et al. (*26*). It has been shown by optical melting studies that the cooperativity in the protein capsid is increasing with the salt concentration between 70 and 200 mM ionic strength, although the phage disruption temperature is not altered.

Effect of Divalent Cations. It is known that DNA−ligand and NP−ligand interactions can be influenced by the presence of metal cations. The strength of these effects increases with the charge of the cation and is substantially larger for transition metal elements.

In our study we investigated the effect of four divalent cations: Mg^{2+}, Ca^{2+}, Cu^{2+}, and Ni^{2+} on TMPyP−DNA and TMPyP−NP binding. Absorption spectra were recorded in 70 mM TRIS buffer completed with 1 mM salt of a divalent cation. Metal complexes of TMPyP were not formed as it was verified by the structure of Q_{xx} and Q_{xy} bands (data not shown). From the spectral analysis concentrations of bound TMPyP species were determined and expressed as the function of base pair/porphyrin molar ratio. Results of spectral analysis are presented in Figures 6 and 7.

As it can be seen from the comparison of data presented in Figure 4A−C and Figure 6A−C, the presence of 1 mM Mg^{2+} or Ca^{2+} does not influence significantly the binding

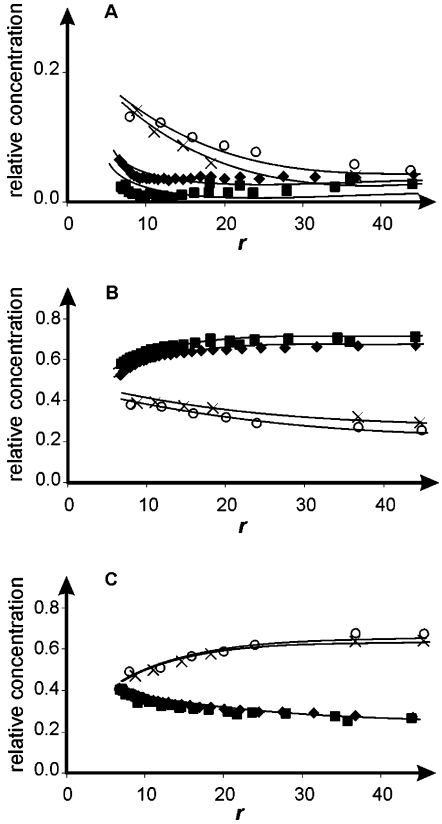

FIGURE 6: Effect of divalent cations on the TMPyP binding to isolated T7 DNA: relative concentration of free (A), intercalated (B), and externally bound (C) TMPyP as a function of the base pair/porphyrin ratio (r). TRIS buffer of 67 mM ionic strength was supplemented with 1 mM Mg^{2+} (■), Ca^{2+} (◆), Cu^{2+} (×), or Ni^{2+} (○) ion.

of TMPyP to DNA. Neither free to bound ratios nor relative concentrations of bound species are altered. We can come to a similar conclusion concerning the effect of these ions on the TMPyP−NP binding (see Figure 5A−C and Figure 7A−C).

Free to bound porphyrin ratios are slightly shifted to the higher values if 1 mM Cu^{2+} and Ni^{2+} are present in a TMPyP−DNA solution. Saturation of binding can be reached around $r = 25$ instead of $r = 10$. However, the contributions of two binding forms are very different in Mg^{2+}/Ca^{2+} or Cu^{2+}/Ni^{2+} containing solution. Both transition metals significantly decrease the binding sites for intercalation and facilitate the groove-binding of TMPyP to isolated DNA.

Comparison of Figure 6 and Figure 7 shows that there is a marked difference between the effects of transient metal ions on TMPyP−DNA or TMPyP−NP interactions. In the case of NP the binding of cationic porphyrin is significantly opposed by 1 mM Cu^{2+} or Ni^{2+}. This originates mainly from the inhibition of intercalation (Figure 7B), but the amount of externally bound species is also slightly reduced, especially by Ni^{2+} (Figure 7C).

All cations tested in this work have the same charge; however, their effects on the TMPyP−DNA or TMPyP−NP binding are not similar. This can be partly interpreted as the result of their different interaction with DNA and NP complex. (*33*). Transition metals interact with nucleobases in DNA, while magnesium and calcium tend to bind almost exclusively to the anionic oxygens of the phosphate groups.

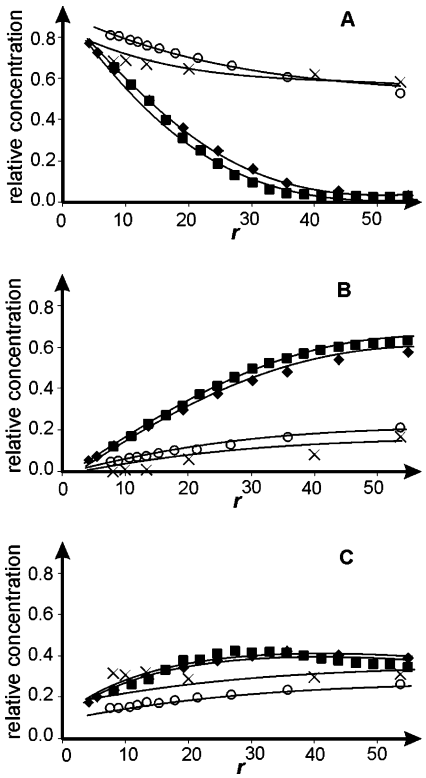

FIGURE 7: Effect of divalent cations on the TMPyP binding to T7 nucleoprotein complex: relative concentration of free (A), intercalated (B), and externally bound (C) TMPyP as a function of the base pair/porphyrin ratio (*r*). TRIS buffer of 67 mM ionic strength was supplemented with 1 mM Mg^{2+} (■), Ca^{2+} (◆), Cu^{2+} (×), or Ni^{2+} (○) ion.

When hydrated Mg^{2+} binds directly to the N7 position of purine bases, the interaction can be viewed as an interaction between nucleobase and a hydrated cation (*34*). It is rather easy to release the Mg^{2+} back to the solvent, but ions of transition metals in the same position establish a considerably stronger interaction with N7 while weakening its binding with the hydrating water molecules. Thus, compared to the Ca^{2+}/Mg^{2+} binding, the hydrated Cu^{2+}/Ni^{2+}−nucleobase complex is shifted considerably to what could be described as hydration of a metalated base. Once bound to N7, it is more difficult to separate Cu^{2+}/Ni^{2+} away from this position, compared to Ca^{2+}/Mg^{2+}.

Spectroscopic evidence has shown (*35*) that in the case of Cu^{2+} and Ni^{2+} if the metal/DNA phosphate molar ratio exceeds 0.4, chelate formation takes place between the N7 of guanines in sequences, other than GpG, and the closest phosphates of the same strand. As a result, GC base pairs open, which destabilizes the helix and provides additional binding sites at the N3 position of cytosine. At high Cu^{2+} concentrations, most GC base pairs appear to be disrupted and only those engaged in sandwich complexes in GpG sequences remain stabilized. The DNA at this point behaves as if it consisted of only AT base pairs. No Cu^{2+} binding to adenine or thymine is thought to take place in native DNA and only upon thermal disruption of AT base pairs Cu^{2+} ions can bind to the N1 of adenine.

Under our experimental conditions the $[Cu^{2+}]$/[phosphate] or $[Ni^{2+}]$/[phosphate] ratio was higher than 1. This condition facilitates the chelate formation and induction of GC base pair disruption described above. It is known that only the CpG site can have full TMPyP intercalation, since the thymine methyl group sterically hinders such geometry at TpA sites. Therefore, reduction of intact GC base pairs reduces the sites of TMPyP intercalation in the DNA chain. This can explain the decrease in the relative concentration of intercalated TMPyP and parallel increase of externally bound species when the buffer solution is supplemented with 1 mM Cu^{2+} and Ni^{2+} ion.

The inhibition of intercalation resulting from Cu^{2+} and Ni^{2+} ion is even more significant in the case of nucleoprotein complex. In this case this phenomenon is not followed by an increase of groove-binding concentration which can be explained by the presence of protein capsid. It has been recently found that the structure of T7 capsid is not destabilized by Cu^{2+} or Ni^{2+} ions; on the contrary, these ions efficiently stabilize the phage proteins (*36*).

CONCLUSION

It was already proven by several studies that the concentration of monovalent salts and the presence of divalent cations even at relatively low concentration influence the interaction between cationic porphyrins and nucleic acids. Most of those results were achieved by the investigation of homologue DNA sequences in binding studies. Even if a natural DNA was selected, the methods used previously measured the bound to free porphyrin ratios, not the distribution between different binding forms. The interaction of cationic porphyrins with natural nucleoprotein complex was never quantitatively investigated before.

In the present study we determined the quantity of two main binding forms of TMPyP under various experimental conditions, and also compared the effect of salts on TMPyP−DNA and TMPyP−NP interactions. This was facilitated by the analysis of TMPyP absorption spectra and the spectral characteristics determined by comprehensive spectroscopic methods in our previous study.

The results presented here fit to the earlier investigations as far as the overall binding process is concerned. However, it became clear that very different variations in the concentrations of the two binding forms can lead to a certain change in the bound TMPyP concentration, or that a constant bound TMPyP concentration can be the result of a significant redistribution of TMPyP molecules between the main binding states. This knowledge is of interest to applications of the cationic porphyrins whenever the binding site of the molecule can influence the mechanism of action or the efficiency of a process (*37*−*39*).

It has been also shown that the structure of protein complex has an important role in the TMPyP−NP interaction, even if there is no direct binding between TMPyP and the proteins (*24*). The spectral parameters of bound TMPyP are very sensitive for the loosening of capsid structure and the consequent conformational changes in target DNA. Based on this observation TMPyP binding can be used as a good indicator of structural integrity of the nucleoprotein complex.

ACKNOWLEDGMENT

We are very grateful to Professor Professor J. Langowski for careful reading of the manuscript and to Erzsebet Szakacs for her technical assistance.

REFERENCES

1. Fiel, R. J., Howard, J. C., and Datta Gupta, N. (1979) Interaction of DNA with a porphyrin ligand: evidence for intercalation, *Nucl. Acids Res. 6*, 3093−3118.
2. Pasternack, R. F., Gibbs. E. J., and Villafranca, J. J. (1983) Interactions of porphyrins with nucleic acids, *Biochemistry 22*, 2406−2414.
3. Sehlstedt, U., Kim, S. K., Carter, P., Goodisman, J., Vollano, J. F., Norden, B., and Dabrowiak, J. C. (1994) Interaction of cationic porphyrins with DNA, *Biochemistry 33*, 417−426.
4. Kelly, J. M., Murphy, M. J., McConnell, D. J., and Uigin, C. (1985) A comparative study of the interaction of 5,10,15,20-tetrakis(N-methylpyridinium-4-yl)porphyrin and its zinc complex with DNA using fluorescence spectroscopy and topoisomerisation, *Nucleic Acids Res. 13*, 167−184.
5. Shen, Y., Myslinski, P., Treszczanovicz, T., Liu, Y., and Koningstein, J. A. (1992) Picosecond laser-induced fluorescence polarization studies of mitoxantrone and tetrakisporphine/DNA complexes, *J. Phys. Chem. 96*, 7782−7787.
6. Geacintov, N. E., Ibanez, V., Rougee, M., and Bensasson, R. V. (1987) Orientation and linear dichroism characteristics of porphyrin-DNA complexes, *Biochemistry 26*, 3087−3092.
7. Sari, M. A., Battioni, J. P., Mansuy, D., and Le-Pecq, J. B. (1986) Mode of interaction and apparent binding constants of meso-tetraaryl porphyrins bearing between one and four positive charges with DNA, *Biochem. Biophys. Res. Commun. 141*, 643−649.
8. Hui, X., Gresh, N., and Pullman, B. (1990) Modelling of the binding specificity in the interactions of cationic porphyrins with DNA, *Nucleic Acids Res. 18*, 1109−1114.
9. Ford, K. G., and Neidle, S. (1995) Perturbations in DNA structure upon interaction with porphyrins revealed by chemical probes, DNA footprinting and molecular modelling, *Bioorg. Med Chem. 3*, 671−677.
10. Ford, K. G., Pearl, L. H., and Neidle, S. (1987) Molecular modelling of the interactions of tetra-(4-N-methylpyridyl) porphin with TA and CG sites on DNA, *Nucleic Acids Res. 15*, 6553−6562.
11. Fiel, R. J. (1989) Porhpyrin−nucleic acid interactions: a review, *J. Biomol. Struct. Dyn. 6*, 1259−1273.
12. Merchat, M., Bertolini, G., Giacomini, P., Villanueva, A., and Jori, G. (1996) Meso-substituted cationic porhpyrins as efficient photosensitizers of Gram-positive and Gram-negative bacteria, *J. Photochem. Photobiol., B: Biol. 32*, 153−157.
13. Trannoy, L. L., Lagerberg, J. W. M., Dubbelman, T. M. A. R., Schuitmaker, H. J., and Brand, A. (2004) Positively charged Porphyrins: a new series of photosensitizers for sterilization of red blood cell concentrates, *Transfusion 44*, 1186−1196.
14. Fedoroff, O. Y., Rangan, A., Chemeris, V. V., and Hurley, L. H. (2000) Cationic porphyrins promote the formation of i-motif DNA and bind peripherally by a nonintercalative mechanism, *Biochemistry 39*, 15083−15090.
15. Weisman-Shomer, P., Cohen, E., Hershco, I., Khateb, S., Wolfovitz-Barchad, O., Hurley, L. H., and Fry, M. (2003) The cationic porphyrin TMPyP4 destabilizes the tetraplex form of the fragile X syndrome expanded sequence d(CGG)n, *Nucleic Acids Res. 31*, 3963−3970.
16. Verma, A., and Rotello, V. M. (2005) Surface recognition of biomacromolecules using nanoparticle receptors, *Chem. Commun. 2*, 303−312.
17. Goodman, C. M., McCusker, C. D., Yilmaz, T., and Rotello, V. M. (2004) Toxicity of Gold Nanoparticles Functionalized with Cationic and Anionic Side Chains, *Bioconjugate Chem. 15*, 897−900.
18. Pasternack, R. F., Garrity, P., Ehrlich, B., Davis, Ch. B., Gibbs. E. J., Orloff, G., Giartosio, A., and Turano, C. (1986) The influence of ionic strength on the binding of water soluble porphyrin to nucleic acid, *Nucleic Acids Res. 14*, 5919−5931.
19. Strickland, J. A., Marzilli, L. G., Gay, K. M., and Wilson, W. D. (1988) Porphyrin and metalloporphyrin binding to DNA polymers: rate and equilibrium binding studies, *Biochemistry 27*, 8870−8878.
20. Dougherty, G., and Pasternack, R. F. (1992) Base pair selectivity in the binding of copper (II) tetrakis 4-N-methylpyridyl) porphine to polynucleotides under closely packed conditions, *Biophys. Chem. 44*, 11−19.
21. Chirvony, V. S., Galievsky, V. A., Kruk, N. N., Dzhagarov, B. M., and Turpin, P. (1997) Photophysics of cationic 5,10,15,20-tetrakis(4-N-methylpyridiniumyl)porphyrin bound to DNA, [poly(dA-dT)]2 and [poly(dG-dC)]2: on a possible charge transfer process between guanine and porphyrin in its excited singlet state, *J. Photochem. Photobiol., B: Biol. 40*, 154−162.
22. Sari, M. A., Battioni, J. P., Dupre, D., Mansuy, D., and Le-Pecq, J. B. (1990) Interaction of cationic porphyrins with DNA: importance of the number and position of the charges and minimum structural requirements for intercalation, *Biochemistry 29*, 4205−4215.
23. Tjahjono, D. H., Akutsu, T., Yoshioka, N., and Inoue, H. (1999) Cationic porphyrins bearing diazonium rings, synthesis and their interaction with calf thymus DNA, *Biochim. Biophys. Acta 1472*, 333−343.
24. Zupan, K., Herényi, L., Toth, K., Majer, Zs., and Csik, G. (2004) Binding of cationic porphyrin to isolated and encapsidated viral DNA analyzed by comprehensive spectroscopic methods, *Biochemistry 43*, 9151−9159.
25. Strauss, J. H., and Sinsheimer, R. L. (1963) Purification and properties of bacteriophage MS2 and of its ribonucleic acids, *J. Mol. Biol. 7*, 43−48.
26. Toth, K., Csik, G., and Ronto, Gy. (1987) Salt effects on the bacteriophage T7- II. Structure and activity changes, *Physiol. Chem. Phys. Med. NMR. 19*, 67−74.
27. Fekete, A., Vink, A. A., Gaspar, S., Berces, A., Modos, K., Ronto, G., and Roza, L. (1998) Assessment of the effects of various UV sources on inactivation and photoproduct induction in phage T7 dosimeter, *Photochem. Photobiol. 68*, 527−531.
28. Serwer, P. (1978) A technique for observing extended DNA in negatively stained specimens: observation of bacteriophage T7 capsid-DNA complexes, *J. Ultrastruct. Res. 65*, 112−118.
29. Toth, K., Bolard, J., Ronto, G., and Aslanian, D. (1984) UV-induced small structural changes in the T7 bacteriophage studied by melting methods, *Biophys. Struct. Mech. 10*, 229−239.
30. Fekete, A., Ronto, G., Feigin, L. A., Tikhonychev, V. V., and Modos, K. (1982) Temperature-dependent structural changes of intraphage T7 DNA, *Biophys. Struct. Mech. 9*, 1−9.
31. Kuroda, R., and Tanaka, H. (1994) DNA-porphyrin interactions probed by induced CD spectroscopy, *J. Chem. Soc., Chem. Commun. 13*, 1575−1576.
32. Tóth, K., and Rontó, Gy. (1987) Salt effects on the bacteriophage T7 − I, *Physiol. Chem. Phys. Med. NMR 19*, 59−66.
33. Šponer, J., Leszczynski, J., and Hobza, P. (2001/2002) Electronic properties, hydrogen bonding, stacking, and cation binding of DNA and RNA bases, *Biopolymers 61*, 3−31.
34. Šponer, J., Burda, J. V., Sabat, M., Leszczynski, J., and Hobza, P. (1998) Interaction between the Guanine-Cytosine Watson−Crick DNA Base Pair and Hydrated Group IIa (Mg^{2+}, Ca^{2+}, Sr^{2+}, Ba^{2+}) and Group IIb (Zn^{2+}, Cd^{2+}, Hg^{2+}) Metal Cations, *J. Phys. Chem. A. 102*, 5951−5957.
35. Tajmir-Riahi, H.-A., Naoui, M., and Ahmad, R. (1993) The effects of Cu2+ and Pb2+ on the solution structure of calf thymus DNA: DNA condensation and denaturation studied by Fourier transform IR difference spectroscopy, *Biopolymers 33*, 1819−1827.
36. Whang, T., Daly, B., and Yin, J. (1996) Metal-ion discrimination by phage T7, *J. Inorg. Biochemistry 63*, 1−7.
37. Lang, K., Mosinger, J., and Wagnerová, D. M. (2004) Photophysical properties of porphyrinoid sensitizers non-covalently bound to host molecules; models for photodynamic therapy, *Coord. Chem. Rev. 248*, 321−350.
38. Wang, G., Zhang J., and Murray R. W. (2002) DNA binding of an ethidium intercalator attached to a monolayer-protected gold cluster, *Anal. Chem. 74*, 4320−4327.
39. Ricchelli, F., Franchi, L., Miotto, G., Borsetto, L., Gobbo, S., Nikolov, P., Bommer, J. C., and Reddi, E. (2005) Meso-substituted tetra-cationic porphyrins photosensitize the death of human fibrosarcoma cells via lysosomal targeting, *Int. J. Biochem. Cell B. 37*, 306−319.

BI0510227